Elastomeric Polypropylenes from Unbridged 2-Phenylindene Zirconocene Catalysts: Temperature Dependence of Crystallinity and Relaxation Properties

Yirong Hu,[†] Eric D. Carlson,[‡] Gerald G. Fuller,*[,‡] and Robert M. Waymouth*[,†]

Department of Chemistry and the Department of Chemical Engineering, Stanford University, Stanford, California 94305

Received August 25, 1998

ABSTRACT: The solid-state structure and physical behavior of an elastomeric polypropylene (PP1) synthesized with unbridged 2-phenylindene zirconocene catalyst were examined using solid-state ^{13}C NMR spectroscopy, differential scanning calorimetry, wide-angle X-ray powder diffraction, and birefringence measurements of relaxation behavior. Extraction of these elastomeric polypropylenes with boiling ether and heptane yielded three fractions of different molecular weight and tacticity. The ether-soluble fraction is the lowest in isotactic pentad content and exhibits no detectable crystallinity. For the other fractions and the parent homopolymer, the degrees of crystallinity estimated from DSC and WAXD results are similar. The amount of the immobile phase determined by solid-state NMR, however, appears much higher than the degree of crystallinity. An increase in temperature from 20 to 80 °C results in a loss in the relative fraction of mobile and immobile phase as measured by solid-state NMR and a corresponding loss in the percent crystallinity as measured by DSC. The relaxation of polymer samples subjected to step shear as a function of increasing temperature was investigated using polarized optical birefringence measurements. These studies revealed that the elastic network remains stable up to temperatures of 80 °C. Blends of atactic and isotactic polypropylene with similar average isotactic pentad contents as PP1 and its heptane-insoluble fraction were examined in comparison. Despite their similar taciticities and degrees of crystallinity, the blends show no evidence of a network structure after being subjected to a step shear but instead relax back to an isotropic orientation.

Introduction

The microstructure of polypropylene has a profound effect on its properties.[1] Isotactic polypropylene is a crystalline thermoplastic whereas atactic polypropylene is amorphous. Elastomeric polypropylene has the properties of a thermoplastic elastomer; the properties of this material were first interpreted by Natta in terms of a stereoblock structure.[1,2] Although not as stable to solvents and high temperatures as their thermoset counterparts, thermoplastic elastomers are a rapidly growing section of the elastomer market due to their low production costs and ease of processing.[3]

In the 1950s, Natta[1,2] first isolated elastomeric polypropylene from a mixture of polypropylenes and assigned a stereoblock structure to this material due to its unique thermal and mechanical properties. Following Natta's efforts, researchers at Dupont[4−6] produced mixtures of polypropylenes that possessed elastomeric properties without fractionation. The first uniform elastic homopolymer of propylene was synthesized by Chien,[7−12] and its stereoblock structure was postulated to be a result of interconversion between isospecific and aspecific sites of the polymerization catalyst.[13−15] Recently, we developed a strategy to synthesize stereoblock polypropylene with an unbridged 2-arylindene metallocene catalyst whose structure was designed to switch between chiral and achiral configurations to produce an isotactic/atactic homopolymer of propylene.[16−23]

Polypropylenes synthesized from 2-arylindene metallocenes were found to be compositionally heterogeneous in terms of tacticity and molecular weight.[24,25] Mechanical tensile tests revealed the elastomeric nature of these materials at room temperature.[16,24] As part of our continuing studies on elastomeric polypropylenes synthesized with unbridged 2-phenylindene zirconocene catalysts, we now report the solid-state structure and temperature-dependent physical behavior of elastomeric propylene homopolymer PP1 and its fractions. To probe the influence of temperature on the percent crystallinity as well as the relaxation behavior, studies were carried out at specific temperatures across the melting profile (20, 50, and 80 °C). The amount of mobile and immobile phases in these materials was investigated by solid-state ^{13}C NMR spectroscopy. Information regarding the level and type of chain organization in the solid state were collected using wide-angle X-ray powder diffraction (WAXD), and the thermal properties were investigated by differential scanning calorimetry (DSC). Relaxation behavior following large-amplitude step-shear deformation was examined with dynamic birefringence measurements.[26,27] In addition, tacticity-matched isotactic/atactic blends were also compared to investigate the role of connectivity in the presumed stereoblock structure of the homopolymers.

Results

PP1 Characterization. The elastomeric propylene PP1 was produced with the unbridged metallocene bis(2-phenylindenyl)zirconium dichloride/MAO at 23 °C from liquid propylene.[24,25] As shown in Table 1, PP1 has a molecular weight of 455 000 and a molecular weight distribution $M_w/M_n = 2.7$. The microstructure was analyzed in solution by ^{13}C NMR and reported in terms of the isotactic pentad content which is the fraction of five contiguous isotactic stereosequences in the poly-

[†] Department of Chemistry.
[‡] Department of Chemical Engineering.

10.1021/ma981336k CCC: $18.00
Published on Web 04/30/1999

Table 1. Microstructure and Thermal Properties

sample	mmmm[a]	M_w[b] ($\times 10^{-3}$)	M_w/M_n	T_m (°C)	ΔH_f (J/g)	$\Delta H_{f(aged)}$ (J/g)
PP1	0.32	455	2.7	138.1	24	24
PP1-ES	0.18	339	2.5			
PP1-HS	0.33	367	2.4	79.7	11	35
PP1-HI	0.51	598	3.1	141.6	65	73
B41	0.33			130.6	24	24
B374	0.57			142.4	48	48

[a] Determined by ^{13}C NMR, the fraction of five contiguous isotactic stereosequences in the polymer. [b] Determined by GPC (waters 150C) at Amoco Chemical Co.

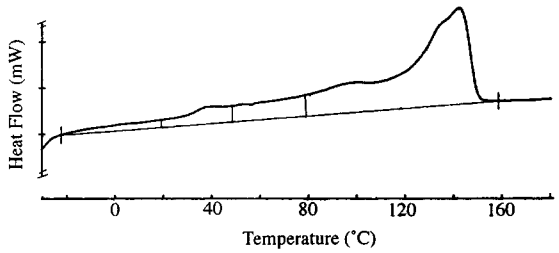

Figure 1. DSC of heptane-insoluble fraction of PP1. The area under the endotherm is divided into partial areas with boundaries set at 20, 50, and 80 °C.

Table 2. Degree of Crystallinity

		degree of crystallinity (%)					
sample	temp (°C)	SS NMR[a]	SS NMR[b]	% loss[c]	DSC[d]	% loss[e]	X-ray
PP1	20	47	59		11		15
	50	34	46		9	18	
	80	24	40	20	7	22	
PP1-HS	20	52	59		15		13
	50	46	40		11	27	
	80	32	27	30	7	36	
PP1-HI	20	60	74		33		22
	50	52	56		30	9	
	80	32	37	35	25	17	
B41	20	41	46		11		22
	50	37	31		11	0	
	80	21	27	29	11	0	
B374	20	66	81		23		36
	50	51	75		23	0	
	80	38	55	25	23	0	

[a] Using Saito's method. [b] Using Zeigler's method. [c] Loss in crystallinity from 50 to 80 °C by solid-state NMR (average of the two methods). [d] Since $\Delta H = 209$ J/g for 100% crystalline polypropylene, % crystallinity $= \Delta H_f$(aged)/209. [e] Loss in crystallinity from 20 to 50 °C and from 50 to 80 °C.

mer.[28] PP1 has an isotactic pentad content of 32%.[24,25,29] Thermal analysis of PP1 was carried out by differential scanning calorimetry. In the DSC studies, two melting peaks ($T_{m1} = 39$ °C; $T_{m2} = 138$ °C) and a broad melting endotherm that spans the temperature range from −20 to 165 °C were observed. The degree of crystallinity in PP1 was found to be approximately 11% by dividing its enthalpy of fusion by 209 J/g.[30,31] To estimate the degree of crystallinity in the sample at different temperatures, the area under the melting endotherm was divided into partial areas, with the boundaries set at 20, 50, and 80 °C on the temperature axis (Figure 1). As seen in Table 2, accompanying the increase in temperature, there is a corresponding decrease in the degree of crystallinity, as estimated by DSC.

The X-ray diffraction pattern shows reflections at $2\theta = 14.0°$, 16.8°, 18.6°, 21.1°, and 21.7° (Figure 2). These are characteristic reflections of the α crystalline phase[32,33]

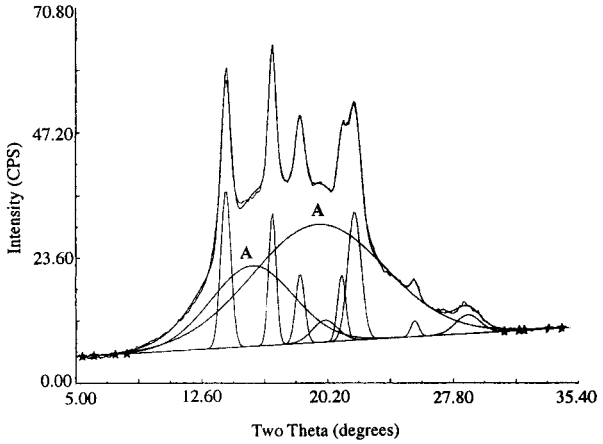

Figure 2. Deconvoluted X-ray diffraction pattern of heptane-insoluble fraction of PP1. The peaks labeled with "A" are amorphous background, and the other peaks are crystalline reflections.

of polypropylene. By fitting the diffraction pattern to five crystalline and two amorphous peaks, the percent crystallinity can be estimated and is reported in Table 2.[31] At room temperature, the degree of crystallinity estimated from WAXD is similar to that estimated from DSC.

High-resolution solid-state ^{13}C NMR experiments were carried out at 20, 50, and 80 °C on a Unity-Inova 300 spectrometer. The experiments were based on two recent studies by Zeigler[34] and Saito,[35] both of which employed direct excitation to determine the amount of mobile and immobile fractions in polypropylene. A delay time of 240 s was chosen for PP1.[36] The room-temperature spectrum showed three broad peaks corresponding to the methylene, methine, and methyl carbons in polypropylene (Figure 3). As temperature increases, the resolution improves, and at 80 °C, both the methylene and the methine signals split into two resonances, which were then deconvoluted into component peaks with Lorentzian line shapes using the Felix program.[37] For the methylene resonances, the peak centered at 46.4 ppm was attributed to the mobile phase and the peak centered at 44.8 ppm to the immobile phase.[35] For the methine resonances, the peak centered at 28.8 ppm was attributed to the mobile phase and the peak centered at 26.6 ppm to the immobile phase.[35] Upon integrating the area under each component peak, the immobile fraction (related to crystallinity) in PP1 was then calculated using two methods. Saito's method[35] involves division of the area under the immobile component of the methylene resonance by the total area of the doublet. Zeigler's approach,[34] on the other hand, assumes the area under the methyl resonance is invariant with temperature and estimates the percentage of the mobile phase from the ratio between the area under the methine resonance at 28.8 ppm and the area under the methyl resonance. Subtracting this ratio from 100% gives an estimate for the immobile fraction. Table 2 summarizes the solid-state NMR, DSC, and X-ray analysis results.

The elastomeric properties of PP1 were probed by monitoring the time-dependent birefringence following large-amplitude step-shear deformations.[26,27] Using the optical train illustrated in Figure 4, birefringence arising from orientations in the 1−3 flow−vorticity plane were measured. Polypropylene has a positive stress−

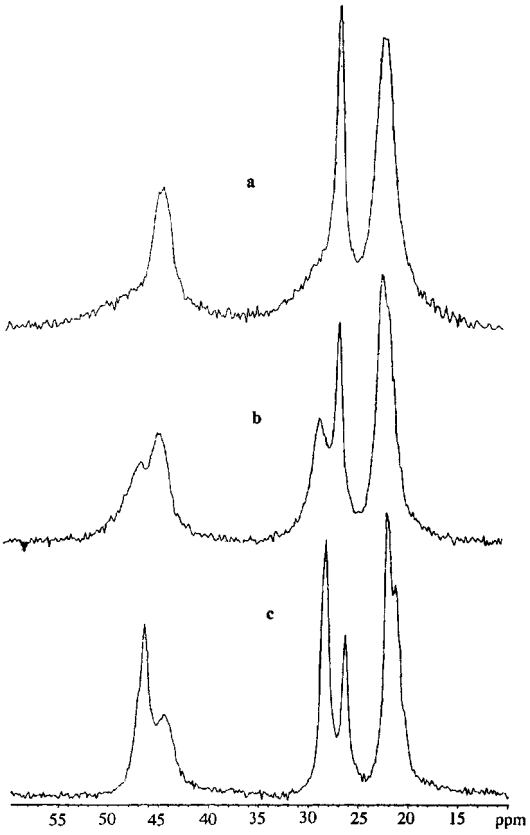

Figure 3. ^{13}C MAS single-pulse excitation (delay time = 240 s) spectra of heptane-insoluble fraction of PP1 (a) at 20 °C, (b) at 50 °C, and (c) at 80 °C.

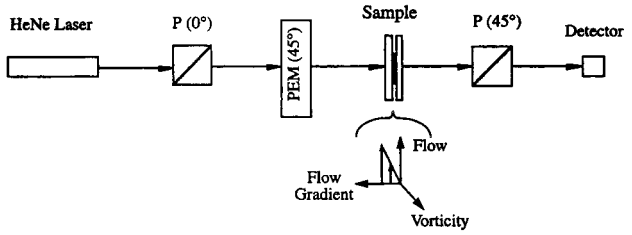

Figure 4. Birefringence optical train.

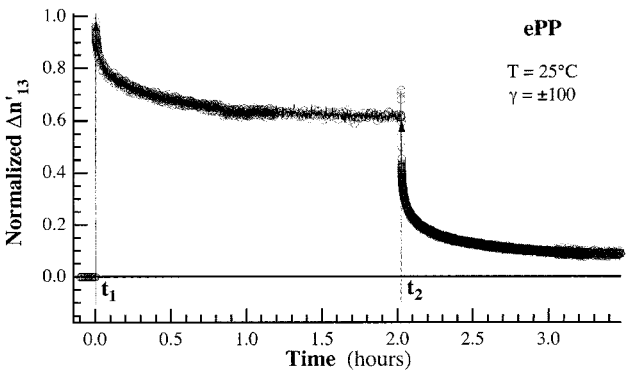

Figure 5. PP1 under 100% step shear. Deformed at $T = 25$ °C.

optical coefficient, so a positive birefringence signal signifies polymer chains oriented in the flow direction. Figure 5 shows the birefringence response of PP1 normalized with its maximum value plotted against time for a reversed step-shear experiment carried out at 25 °C and 100% shear. From an initially quiescent, zero-birefringence state, deformation at t_1 caused the birefringence to step up to a positive value. Immediately

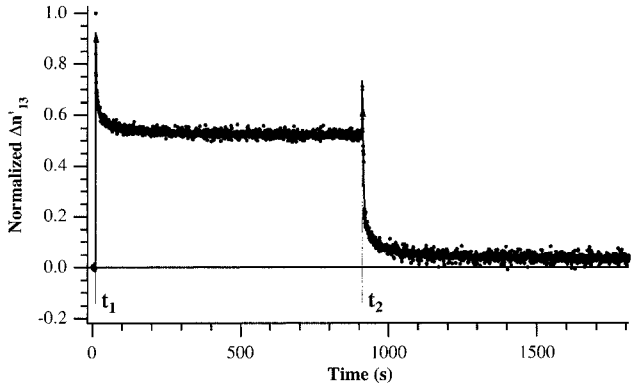

Figure 6. PP1 under 100% step shear. Deformed at $T = 80$ °C.

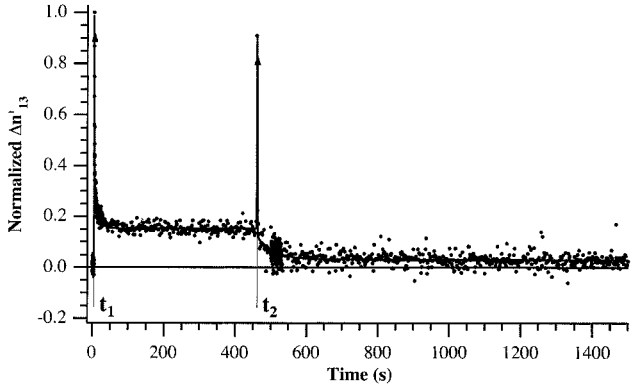

Figure 7. PP1 under 100% step shear. Deformed at $T = 115$ °C.

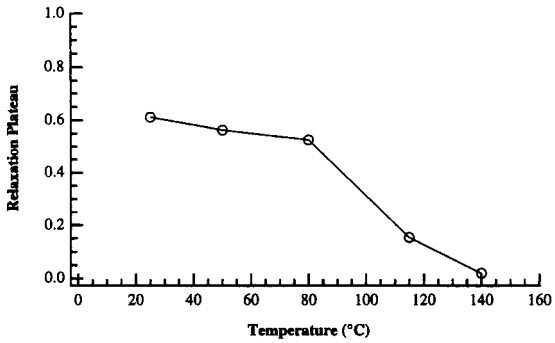

Figure 8. PP1 relaxation plateau as a function of temperature.

following the deformation, the signal decayed monotonically. In contrast to atactic polypropylene or other amorphous polymer melts, this system did not relax to an isotropic, zero-birefringence state;[26] rather, the signal relaxes to a nonzero plateau value. This behavior is indicative of an elastic network that maintains some degree of orientation at constant deformation. At t_2 the deformation was reversed, and the birefringence signal relaxes toward an isotropic state. The birefringence responses of PP1 at 80 and 115 °C are shown in Figures 6 and 7. The birefringence signals at these temperatures also stepped to a positive value upon deformation and then decayed to a plateau. In Figure 8, the plateau level as a percentage of the maximal birefringence was plotted against temperature. Deformation at 25 °C led to a plateau value of 0.62; thus, 62% of the flow-induced optical anisotropy was unable to relax in this sample. This plateau persisted up to 80 °C, at which temperature deformation led to a birefringence of 0.43. At 115

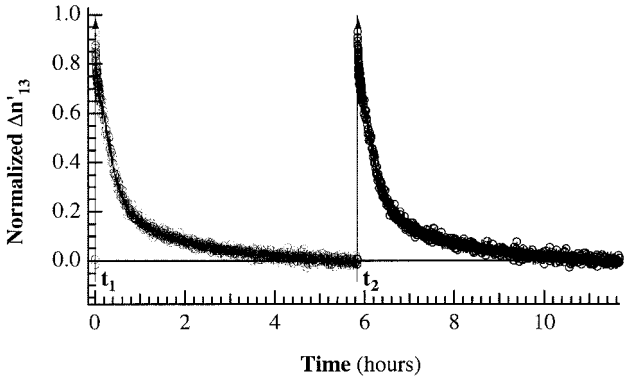

Figure 9. B41 under 100% step shear. Deformed at $T = 25$ °C.

°C, the level of the relaxation plateau fell off, and the system had a residual birefringence of 0.15 following deformation. Complete relaxation of the deformed sample was achieved at 140 °C.

Isotactic/Atactic Blends. Blend B41 was prepared to have the same average isotactic pentad content as PP1 ([mmmm] = 0.33) by mixing 0.89 g of isotactic polypropylene and 2.11 g of atactic polypropylene in boiling xylene. DSC studies of B41 showed a much narrower melting endotherm than that of the elastomeric homopolymer PP1.[25] The onset of melting was observed at 90 °C; thus, there is no change in crystallinity as temperature increases from 20 to 80 °C. Only one melting peak was found at 131 °C. The X-ray diffraction patterns and solid-state ^{13}C NMR spectra of B41 and PP1 look very similar. Analysis by WAXD and DSC revealed similar degrees of crystallinity for B41 and PP1 at room temperature. The percentage of immobile phase measured for B41 by solid-state NMR was slightly less than that of PP1; nevertheless, the measured loss in percentage of the immobile phase was greater for B41 between 50 and 80 °C (Table 2). Dynamic birefringence studies of B41 were carried out at 25 °C (Figure 9). In contrast to PP1, deformation at t_1 led to a nonzero birefringence which then relaxed to an isotropic state after 2 h. Reversal of deformation at t_2 led to a similar response since the material had relaxed to an isotropic state.

Blend B374 was made by solution polymerization in toluene with a catalyst mixture containing both *rac*- and *meso*-dimethylsilylbis(2-phenylindenyl)zirconium dichloride (rac/meso = 2.95).[38,39] B374 has a molecular weight $M_w = 374\,000$ and a molecular weight distribution $M_w/M_n = 3.9$. Its thermal behavior and phase structure were compared to those of the heptane-insoluble fraction of PP1, which has a similar isotactic pentad content.

Fractionation. Homopolymer PP1 can be separated into fractions that differ in their solubilities in boiling ether and heptane.[24,25,29] The three fractions PP1 yielded are ether-soluble (ES), heptane-soluble (HS), and heptane-insoluble (HI) fractions. The ES fraction is the lowest in isotactic pentad content ([mmmm] = 0.18) while HI fraction is the highest ([mmmm] = 0.51). The ES and HS fractions have similar molecular weights and molecular weight distributions, while the HI fraction has a higher molecular weight and a broader molecular weight distribution ($M_w/M_n = 3.1$). No thermal transitions were observed for the ES fraction by DSC. Both the HS and HI fractions exhibited very broad melting endotherms similar to the parent homopolymer. A peak melting point at 80 °C was found for the HS fraction while two peaks at 37 and 142 °C were observed for the HI fraction. Compared to the HS fraction, the HI fraction appears to have a higher degree of crystallinity and less crystallinity loss during heating (by DSC). The solid-state ^{13}C NMR results showed, however, the percent loss in the immobile fraction as a function of temperature is approximately the same for these two fractions.

Compared to the HI fraction, blend B374 exhibited a narrower melting transition. The DSC crystallinity in B374 remained the same before temperature reached 90 °C. A single melting peak was observed at 142 °C. As in the studies where B41 was compared to PP1, a striking resemblance was also found in the X-ray diffraction patterns and the ^{13}C NMR spectra of B374 and the HI fraction. The fractions of the immobile phases in these two samples measured by solid-state NMR at room temperature were similar and appeared to yield a similar percent loss with increasing temperature. The relaxation behavior of the fractions at room temperature is reported elsewhere.[26]

Discussion

For semicrystalline homopolymers, crystallites are typically associated with interfacial and amorphous regions.[40−42] The crystallites can be organized, under certain circumstances, into higher levels of morphology or supermolecular structure such as spherulites and related forms.[43] The rate and extent of crystallization defines the total amount of crystalline material present as well as the size and shape of the crystalline domains, which then in turn have a profound influence on the physical and mechanical properties. Differential scanning calorimetry, wide-angle X-ray powder diffraction, and solid-state ^{13}C NMR are three techniques that can shed light on the crystallite size and stability, the nature of the crystalline phases, and the degree of crystallinity. Due to the complexity in the structure and organization of semicrystalline polymers, the degree of crystallinity is often difficult to measure.[31] It is frequently observed that the crystallinities measured by various methods are not all consistent with each other. With the above in mind, we probed the solid-state structure of the elastomeric propylene homopolymer PP1 and its fractions using these three techniques. The physical behavior was examined with dynamic birefringence experiments. Blends with similar average isotactic pentad contents to PP1 and its HI fraction were also studied in comparison.

PP1 was synthesized with bis(2-phenylindenyl)zirconium dichloride/MAO from liquid propylene at 23 °C. Previous studies on PP1 have demonstrated that it has a slower crystallization rate than B41.[25] This is evidenced in our DSC studies by the appearance of a second melting peak at 45 °C after PP1 had been aged for a day. On the other hand, aging showed no observable effect on the thermal behavior of B41. This suggests that the slower crystallization of PP1 might be associated with its blocky structure. The broad melting endotherm observed for PP1 is indicative of a distribution of crystallite sizes and stabilities. Accompanying the rise in temperature, there is a substantial loss in PP1's degree of crystallinity. In contrast, B41 showed a much narrower melting endotherm, and the degree of crystallinity remained invariant below 90 °C. X-ray diffraction studies revealed both PP1 and B41 are dominated by the α crystalline phase. The degrees of

crystallinity estimated from X-ray analysis are consistent with those from DSC analysis and indicate that PP1 and B41 have similar degrees of crystallinity at room temperature.

The relative percentages of mobile and immobile phases measured by solid-state NMR are also similar for PP1 and B41. For both samples, there is a large discrepancy between the degree of crystallinity measured by DSC and WAXD and the percentage of immobile phase measured by solid-state NMR. The origin of this discrepancy is not clear but is likely a consequence of the presence of multiple phases of varying order present in these low-crystallinity semicrystalline elastomers. The broad line widths observed in the room-temperature solid-state NMR spectra (Figure 3a) lead to considerable uncertainty in the estimates of the percent immobile phase. Despite these difficulties, the solid-state NMR results, when combined with the DSC analysis, are useful methods for monitoring the loss in crystallinity with increasing temperature. Both the solid-state NMR results and the DSC results reveal that a percentage of crystalline or immobile phase is retained in sample PP1 at temperatures up to 80 °C.[44]

While the WAXD, DSC, and solid-state NMR provide evidence for similar degrees of crystallinity for PP1 and B41, large differences were observed in their relaxation behavior following step shear. In the dynamic birefringence studies, PP1 did not completely relax following step-shear deformation while B41 relaxed to a zero-birefringence, isotropic state. Clearly, the PP1 was able to form semipermanent physical cross-links and create a thermoplastic elastomeric network. In addition, the persistence of the PP1 relaxation plateau with increasing temperature (Figure 8) indicates that PP1 remains a thermoplastic elastomer at temperatures well into the melting profile. The changes that are evident by DSC and solid-state NMR have only a minor effect on the elastomeric nature of the sample up to 80 °C. One possible explanation is that the crystallites that melt below 80 °C do not contribute significantly to the elastic network; thus, their melting has a negligible effect on the relaxation properties. Another possibility is that the low-temperature meltings are the result of the crystallites melting, re-forming, and annealing. Crystallites involved in the cross-link structure may undergo transitions and the morphology of the cross-link may change, but the physical cross-links persist.

The compositional heterogeneity of PP1 was investigated by fractionation in refluxing ether and heptane. Fractionation of PP1 yielded ether-soluble, heptane-soluble, and heptane-insoluble fractions.[24−26] Among them, ES fraction is the lowest in isotactic pentad content ([mmmm] = 0.32) while HI fraction is the highest ([mmmm] = 0.51). Molecular weights of the ES and HS fractions are reasonably close to that of PP1. The HI fraction has the highest molecular weight and the broadest molecular weight distribution (M_w/M_n = 3.1). Broad melting endotherms were observed in the DSC studies of HS and HI fractions, suggesting a distribution of crystallite sizes and stabilities. X-ray patterns of these two fractions exhibited α and γ crystalline phases. In contrast, the ES fraction showed no thermal transitions or crystalline reflections. Deconvolution of the solid-state NMR spectra of the ES fraction was also unsuccessful.

For HS and HI fractions, the degree of crystallinity estimated from DSC and that from X-ray are reasonably close. Similar to PP1, the immobile fractions of these two samples (by solid-state NMR) are also approximately 40% higher than their degrees of crystallinity. The percent loss in immobile phase is comparable for the HS and HI fractions. However, the HS fraction suffers from a greater loss in degree of crystallinity (by DSC) than the HI fraction (26% vs 15%) accompanying the increase in temperature from 50 to 80 °C.

The differing levels of crystallinities among the various fractions[24] would be expected to lead to distinct physical behavior for each fraction. A key question is whether the physical properties of the whole polymer is a linear combination of the properties of the fractions or whether there is some cooperative behavior of the various fractions that lead to unique properties when combined. This is the subject of ongoing investigations in our laboratories. An investigation of the tensile properties of the fractions as well as the component behavior of the fractions within the elastomeric polypropylene sample is underway and will be reported elsewhere.[26,27,45]

The total amount of crystallinity or immobile phase in the atactic/isotactic blends was approximately equal to that of the elastomeric polypropylenes of similar average structure: blend B374 has a similar isotactic pentad content as the HI fraction and also appears to have a similar percentage of immobile fractions and degrees of crystallinity. However, the thermal behavior and relaxation properties of these two samples are quite different. Blend B374 had a much narrower melting endotherm, and there was no noticeable change in its degree of crystallinity between 20 and 80 °C as estimated by DSC. The percent loss in the immobile phase of B374 was 10% less than that of HI fraction.

Conclusions

Investigations by WAXD, DSC, solid-state NMR, and rheooptical methods at room temperature reveal that polypropylenes prepared with 2-arylindene catalysts are semicrystalline materials which exhibit the behavior of an elastomeric network when subjected to a step shear. In contrast, blends of isotactic and atactic polypropylenes relax to an isotropic orientation following a step shear. The crystalline phases of the elastomeric polypropylenes are characterized by a very broad melting endotherm. Studies by DSC and solid-state NMR demonstrate a considerable (approximately 20%) loss in crystallinity in these materials as the temperature is increased to 80 °C. However, the temperature-dependent relaxation behavior shows that the elastomeric network is retained and only begins to degrade significantly at temperatures greater than 80 °C. These results suggest that the lower melting crystalline phases in these thermoplastic elastomers contribute less to the elastomeric network than the higher melting crystallites. The implication of these observations is that these thermoplastic elastomeric polypropylenes should have excellent high-temperature performance and retain their elastomeric properties even at elevated temperatures.

Experimental Section

Sample Preparation. PP1 was synthesized from bis(2-phenylindenyl)zirconium dichloride/MAO at Amoco Chemical Co. from the bulk using liquid propylene monomer. Details of the synthesis and characterization of this sample have been previously reported.[24]

B41 was prepared from 2.11 g of atactic polypropylene and 0.89 g of isotactic polypropylene by dissolving the two purified polymers in refluxing xylene. Details of the synthesis and characterization of this sample have been reported.[25]

B374 was made with catalyst mixtures containing various ratios of *rac*/*meso*-dimethylsilylbis(2-phenylindenyl)zirconium dichloride.[38,39] The catalyst mixture was prepared by mixing various amounts of the individual isomers in toluene and then degassing the solvent in vacuo. The rac/meso ratio was then measured via NMR integration of the dimethylsilyl protons. A 5×10^{-6} mol sample of the catalyst mixture (rac/meso = 2.95) and 294 mg of MAO were dissolved in 25 mL of toluene. The catalyst was allowed to age for 10 min and then was loaded into a 25 mL two-ended injection tube. Meanwhile, the Parr reactor was evacuated and refilled with argon. After flushing three times with 50 psig of nitrogen, 100 mL of liquid propylene was introduced. The catalyst was injected under 200 psig of nitrogen to bring the total reactor pressure to about 160 psig. The reaction was allowed to proceed for 20 min at 20 °C, and then the reaction was quenched with 15 mL of methanol injected under 200 psig of nitrogen. The reactor was allowed to stir overnight and then was rinsed with methanol and dried in vacuo at 40 °C. By fractionation, the weight percentage of the atactic polymer was determined to be 37% and that of the isotactic polymer was 63%. B374 has molecular weight $M_w = 374\,000$ and isotactic pentad content [mmmm] = 0.57.

Purification. A 500 mL round-bottom flask was charged with xylene (300 mL) and 2,6-di-*tert*-butyl-4-methylphenol (BHT) (1 g). The crude polymer PP1 was dissolved at reflux in this solution under nitrogen. The hot polymer solution was filtered over Celite under vacuum and precipitated into acidified methanol (1% HCl) with vigorous stirring. The rubbery white precipitate was frozen in liquid nitrogen, ground in a blender, washed with acidified methanol (100 mL, 10% HCl), and dried overnight at 60 °C in vacuo.

Fractionation. PP1 was fractionated by successive extraction with boiling ether and heptane under nitrogen. A 500 mL round-bottom flask was charged with solvent (300 mL, w/BHT) and attached to a Kumagawa extractor. The polymer (ca. 8 g) was packed into a thimble layered with a plug of glass wool and capped with filter paper (Whattaman #1). The extractor was wrapped with aluminum foil and heated such that the flushing frequency of the extractor was ca. 4 min. The polymer sample was extracted for 24 h and then precipitated by pouring into acidified methanol (3000 mL, 1% HCl) with vigorous stirring. This process was repeated twice for each solvent, and the thimble with contents was dried using an air flush at room temperature between solvent changes. After extraction procedure with heptane, the heptane-insoluble polymer remaining in the thimble was dried by aspiration at room temperature. The heptane-insoluble fraction was then redissolved in refluxing xylene (300 mL, 1 g of BHT), hot filtered over glass wool with vacuum, and precipitated by addition to acidified methanol (3000 mL, 1% HCl). All of the precipitated samples were frozen using liquid nitrogen, ground in a blender, and washed with acidified methanol (150 mL, 10% HCl) before drying at 60 °C in vacuo.

Thermal Analysis. Differential scanning calorimetry was performed on a Perkin-Elmer DSC 7 with indium as a calibration standard. Polymer samples (0.05 g) were wrapped in aluminum foil and melt pressed at ca. 140 °C using light pressure (<250 psig). The foil-wrapped films (ca. 1 mm thick) were removed from the press, quenched into liquid nitrogen, and peeled from the foil before warming. Disklike samples were punched from the cold films using a standard one-hole paper punch. These samples (0.015 g) were weighed and sealed into an aluminum DSC pan supplied by Perkin-Elmer. Samples were first heated from room temperature to 200 °C at 200 °C/min. After being held at 200 °C for 15 min, they were cooled from 200 to −50 °C at 20 °C/min and were then heated to room temperature at 200 °C/min. The samples were allowed to stand at room temperature for 20 h prior to being scanned from −50 to 200 °C at 20 °C/min. All cycles were repeated three times to ensure reproducibility.

Solid-State NMR. Solid-state high-resolution ^{13}C NMR measurements were carried out on a Varian Unity-Inova 300 spectrometer operating at a field strength of 7 T using a 7 mm CP/MAS probe. The radio frequency of 75.4 MHz was used for the detection of ^{13}C resonance. MAS was carried out at a rate of 3.0−3.5 kHz at room temperature and 3.5−4.0 kHz above room temperature using the VT/MAS system. The chemical shift relative to tetramethylsilane was determined by using the methyl peak at 17.3 ppm of hexamethylbenzene as an internal reference. Conventional direct excitation with decoupling of protons during acquisition (Bloch decay) was performed in all experiments. The decoupler field strength was 62.5 kHz. The parameters used were the following: sweep width, 50 000 Hz; number of transitions, 600; delay time, 240 s; acquisition time, 0.040 96 s; pulse width, 4 μs. The samples were treated on a Mettler hotstage prior to the NMR experiments. After being heated from room temperature to 200 °C and held at 200 °C for 15 min, they were cooled from 200 °C to room temperature at 10 °C/min. When they reached room temperature, the samples were removed from the hotstage and were allowed to stand at room temperature for 20 h. For each sample, a series of NMR experiments were carried out at three different temperatures, 20, 50, and 80 °C, and in that order. It was assumed that, with a delay time of 240 s, no allowance was necessary to account for a possible change in temperature during an experiment due to decoupler heating. After a series was completed, a quick experiment was run at 20 °C to ensure the amount of the immobile phase has not changed during the course of the NMR studies. The spectra analysis were carried out using the Felix program provided by Biosym Technologies, Inc., on a Silicon Graphics workstation.

X-ray Analysis. X-ray powder diffraction patterns were obtained on a Rigaku diffractometer using a Cu Kα sealed beam source collimated with a Soller slit box containing a 5° opening angle and a system of diverging, receiving, and scattering slits with 1300 and 600 μm slit widths, respectively. A graphite monochromator was used. Polymer samples were wrapped in aluminum foil and melt pressed at ca. 140 °C using light pressure (<250 psig). The foil wrapped films (ca. 1 mm thick) were removed from the press, quenched into liquid nitrogen, and peeled from the foil before warming. These films were wrapped in aluminum foil and placed on a Mettler hotstage. After being heated from room temperature to 200 °C and held at 200 °C for 15 min, they were cooled from 200 °C to room temperature at 10 °C/min. When they reached room temperature, the samples were removed from the hotstage and were allowed to stand at room temperature for 20 h. The powder diffraction patterns were measured over an angular range of 5−35° 2θ with an angular increment of 0.1° and a count time of 20 s. Analysis of the diffraction pattterns was accomplished using the Shadow software package provided by Materials Data Inc. of Livermore, CA.

Dynamic Birefringence. Figure 4 shows the optical train used to monitor the time-dependent birefringence in these experiments. In this apparatus, monochromatic light is provided by a HeNe laser. The light passes through a polarizer (0°) and photoelastic modulator (PEM, 45°) to provide elliptically polarized light. The light then passes through the sample along the shear gradient axis. The sample is held in a Linkam shearing apparatus modified to contain a nitrogen environment. A rotational displacement voltage transducer was used to measure applied strains. Samples are deformed in a parallel plate geometry with light propagating down the shear gradient axis. Light is collected through an analyzing polarizer (45°) into a photodiode detector. The signals are demodulated using lock-in amplifiers. The intensity of the transmitted light, I, has the following form:

$$I = I_0[1 + 2J_1(A)\sin(\omega t)\sin(\delta)]/4; \quad \delta = 2\pi d\Delta n'_{13}/\lambda$$

where I_0 is the incident intensity, $J_1(A)$ is the Bessel function, ω is the modulation frequency of the PEM, δ is the retardation of the sample, d is the sample thickness, λ is the wavelength of light (0.6328 μm), and $\Delta n'_{13}$ is the birefringence of the

sample in the flow−vorticity plane. Samples were heated to 200 °C under nitrogen in the flow cell and held for 10 min to erase any thermal or strain history. Samples were then cooled at 20 °C/min to 25 °C and were allowed to age for 20 h. For experiments carried out at above 25 °C samples were subsequently heated at 20 °C/min and allowed to equilibrate for 10 min.

Acknowledgment. We thank the NSF for financial support (CHE-9615699 and DMR-9528636). Dr. L. Bendig of Amoco Chemical Co. is gratefully acknowledged for providing us with the elastomeric polypropylene sample PP1. We also thank Dr. E. Hauptman and Dr. M. D. Bruce for providing the propylene homopolymers used in the preparation of blend B41 and J. Maciejewski-Petoff for providing blend B374. Finally, we thank Dr. M. T. Krejchi and C. D. Shah for fractionation of elastomeric homopolymer PP1.

Supporting Information Available: Tables S1−S6 giving complete listing of solid-state ^{13}C NMR spectra analysis results (using the Felix program provided by Biosym Technologies, Inc.); Tables S7−S12 giving complete listing of X-ray powder diffraction pattern analysis results (using the Shadow software provided by Materials Data, Inc.). This material is available free of charge via the Internet at http://pubs.acs.org.

References and Notes

(1) Natta, G. *J. Polym. Sci.* **1959**, *34*, 531−549.
(2) Natta, G.; Mazzanti, G.; Crespi, G.; Moraglio, G. *Chim. Ind. (Milan)* **1957**, *39*, 275−83.
(3) *Thermoplastic Elastomers: A Comprehensive Review*; Legge, N. R., Holden, G., Schroeder, H. E., Eds.; Hanser Publishers: Munich; New York, 1987.
(4) Collette, J. W.; Tullock, C. W. (Dupont) U.S. Patent 4,335,-225, 1982.
(5) Collette, J. W.; Tullock, C. W.; MacDonald, R. N.; Buck, W. H.; Su, A. C. L.; Harrell, J. R.; Mulhaupt, R.; Anderson, B. C. *Macromolecules* **1989**, *22*, 3851−3858.
(6) Collette, J. W.; Ovenall, D. W.; Buck, W. H.; Ferguson, R. C. *Macromolecules* **1989**, *22*, 3858−3866.
(7) Babu, G. N.; Newmark, R. A.; Cheng, H. N.; Llinas, G. H.; Chien, J. C. W. *Macromolecules* **1992**, *25*, 7400−7402.
(8) Cheng, H. N.; Babu, G. N.; Newmark, R. A.; Chien, J. C. W. *Macromolecules* **1992**, *25*, 6980−6987.
(9) Chien, J. C.; Llinas, G. H.; Raush, M. D.; Lin, G. Y.; Winter, H. H.; Atwood, J. L.; Bott, S. G. *J. Am. Chem. Soc.* **1991**, *113*, 8569−8570.
(10) Lin, Y. G.; Mallin, D. T.; Chien, J. C. W.; Winter, H. H. *Macromolecules* **1991**, *24*, 850−854.
(11) Llinas, G. H.; Dong, S.-H.; Mallin, D. T.; Rausch, M. D.; Lin, Y.-G.; Winter, H. H.; Chien, J. C. W. *Macromolecules* **1992**, *25*, 1242−1253.
(12) Llinas, G. H.; Day, R. O.; Rausch, M. D.; Chien, J. C. W. *Organometallics* **1993**, *12*, 1283−1288.
(13) Gauthier, W. J.; Corrigan, J. F.; Taylor, N. J.; Collins, S. *Macromolecules* **1995**, *28*, 3771−3778.
(14) Gauthier, W. J.; Collins, S. *Macromolecules* **1995**, *28*, 3779−3786.
(15) Gauthier, W. J.; Collins, S. *Macromol. Symp.* **1995**, *98*, 223−231.
(16) Coates, G.; Waymouth, R. M. *Science* **1995**, *267*, 217−219.
(17) Hauptman, E.; Waymouth, R. M.; Ziller, J. W. *J. Am. Chem. Soc.* **1995**, *117*, 11586−11587.
(18) Kravchenko, R.; Masood, A.; Waymouth, R. M. *Organometallics* **1997**, *16*, 3635−3639.
(19) Maciejewski-Petoff, J. L.; Bruce, M. D.; Waymouth, R. M.; Masood, A.; Lal, T. K.; Quan, R. W.; Behrend, S. J. *Organometallics* **1997**, *16*, 5909−5916.
(20) Bruce, M. D.; Coates, G. W.; Hauptman, E.; Waymouth, R. M.; Ziller, J. W. *J. Am. Chem. Soc.* **1997**, *119*, 11174−11182.
(21) Kravchenko, R.; Waymouth, R. M. *Macromolecules* **1998**, *31*, 1−6.
(22) Kravchenko, R.; Masood, A.; Waymouth, R. M.; Myers, C. L. *J. Am. Chem. Soc.* **1998**, *120*, 2039−2046.
(23) Lin, S.; Hauptman, E.; Lal, T. K.; Waymouth, R. M.; Quan, R. W.; Ernst, A. B. *J. Mol. Catal. A* **1998**, 1−11.
(24) Hu, Y.; Krejchi, M. T.; Shah, C. D.; Myers, C. L.; Waymouth, R. M. *Macromolecules* **1998**, *31*, 6908−6916.
(25) Carlson, E. D.; Krejchi, M. T.; Shah, C. D.; Terakawa, T.; Waymouth, R. M.; Fuller, G. G. *Macromolecules* **1998**, *31*, 5343−5351.
(26) Carlson, E. D.; Fuller, G. G.; Waymouth, R. M. *Macromolecules*, submitted for publication.
(27) Carlson, E. D.; Fuller, G. G.; Waymouth, R. M. *Macromolecules*, submitted for publication.
(28) Bovey, F. A. *Chain Structure and Conformation of Macromolecules*; Academic Press: New York, 1982.
(29) The full pentad distribution of this polymer and its fractions have been previously reported (refs 24 and 25).
(30) Wunderlich, B. *Macromolecular Physics*; Academic Press: New York, 1976; Vol. 2.
(31) Isasi, J. R.; Mandelkern, L.; Galante, M. J.; Alamo, R. G. *J. Polym. Sci., Part B: Polym. Phys.* **1999**, *37*, 323−334.
(32) Turner Jones, A.; Aizlewood, J. M.; Beckett, D. R. *Makrol. Chem.* **1964**, 75−81.
(33) Gomez, M. A.; Tanaka, H.; Tonelli, A. E. *Polymer* **1987**, *28*, 2227−2232.
(34) Zeigler, R. *Macromol. Symp.* **1994**, *86*, 213−227.
(35) Saito, S.; Moteki, Y.; Nakagawa, M.; Horii, F.; Kitamaru, R. *Macromolecules* **1990**, *23*, 3256−3260.
(36) A delay time of 240 s was employed by Saito et al. in their direct excitation experiments to determine percent crystallinity in isotactic polypropylene. To ensure all structural components of elastomeric polypropylenes are reproduced in our NMR studies, we compared spectra of PP1−HI obtained using delay times of 240 and 480 s. No detectable difference was found in peak intensity or the number of peaks between the two spectra.
(37) Provided by Biosym Technologies, Inc.
(38) Maciejewski-Petoff, J. L.; Waymouth, R. M. *Polym. Prepr.* **1998**, *39*, 212.
(39) Maciejewski-Petoff, J. L.; Agoston, T.; Lal, T. K.; Waymouth, R. M. *J. Am. Chem. Soc.*, submitted for publication.
(40) Mandelkern, L. *J. Phys. Chem.* **1971**, *75*, 3909−3920.
(41) Mandelkern, L. *Characterization of Materials in Research, Ceramics and Polymers*; Syracuse University Press: Syracuse, 1975.
(42) Mandelkern, L. *Acc. Chem. Res.* **1976**, *9*, 81.
(43) Keith, H. D.; Padden, J. F., Jr. *J. Appl. Phys.* **1964**, *35*, 1286−1296.
(44) It should be noted that the results from these characterizations may be influenced by the different cooling rates used in sample preparation. In the solid-state NMR and WAXD studies, samples were pretreated on a Mettler hotstage. Due to limitations of the hotstage, sample cooling was carried out at a rate of 10 °C/min. A cooling rate of 20 °C/min was used in the DSC and dynamic birefringence studies. Since crystallization rate plays an important role in determining the crystallinity of a material, the different cooling rates may be responsible for some of the differences that we observe. The reasonable agreement between the DSC and WAXD estimates would indicate that the cooling rate is not a major determinant.
(45) Chen, Z.; Myers, C. L.; Waymouth, R. M., manuscript in preparation.

MA981336K